Iodine Adsorption Studies of Dipalladium-based Supramolecular Cages①

LU Hong-Lin[a] TONG Jin[a]
MA Hong-Wei[b②] YU Shu-Yan[a②]
[a] (*Laboratory for Self-assembly Chemistry, Department of Environment and Life, Beijing University of Technology, Beijing* 100124, *China*)
[b] (*Analysis and Testing Center, Beijing Institute of Technology, Beijing* 102488, *China*)

ABSTRACT Four water-soluble cage-like hosts (**1·4NO$_3^-$**: {[(bpy)$_2$Pd$_2$]$_2$L$^1_2$}(NO$_3$)$_4$, **2·4NO$_3^-$**: {[(bpy)$_2$Pd$_2$]$_2$L$^2_2$}(NO$_3$)$_4$, **3·6NO$_3^-$**: {[(bpy)$_2$Pd$_2$]$_3$L$^3_2$}(NO$_3$)$_6$ and **4·6NO$_3^-$**: {[(bpy)$_2$Pd$_2$]$_3$L$^4_2$}(NO$_3$)$_6$) have been successfully self-assembled by coordinating the flexible amide based polypyrazole ligands (H$_2$L^1: N^1,N^4-di(1H-pyrazol-5-yl)terephthalamide, H$_2$L^2: N^1,N^4-bis(3-methyl-1H-pyrazol-5-yl)-terephthalamide, H$_3$L^3: N^1,N^3,N^5-tri(1H-pyrazol-5-yl)benzene-1,3,5-tricarboxamide and H$_3$L^4: N^1,N^3,N^5-tris(3-methyl-1H-pyrazol-5-yl)benzene-1,3,5-tricarboxamide) with dipalladium corners ([(bpy)$_2$Pd$_2$(NO$_3$)$_2$](NO$_3$)$_2$, where bpy = 2,2′-bipyridine) in aqueous solution. Their structures were characterized by ^{1}H NMR, ESI-MS and single-crystal X-ray diffraction. Notably, all the four supramolecular assemblies are capable of adsorbing iodine molecules via halogen bonds and other supramolecular interactions.

Keywords: self-assembly, palladium, cages, host-guest, iodine adsorption;
DOI: 10.14102/j.cnki.0254-5861.2011-3271

1 INTRODUCTION

The coordination-driven supramolecular assembly has proven to be one of the most well-established and powerful bottom-up tools capable of not only constructing well-defined and highly ordered two- or three-dimensional supramolecular architectures with robust and directional metal-ligand coordinative bonding[1-7], but also, very often, imparting cation- or anion-sensing functionality to the materials due to the involvement of these ions as the bridging modules[8-13]. Host-guest systems are organized by the type of noncovalent interactions including a wide range of attractive and repulsive forces such as ion-ion interactions, van der Waals forces, ion-dipole interactions, dipole-dipole interactions, hydrogen bonds, halogen bonds, π-π interactions, cation-π, anion-π interactions and so on[14-16]. In order to form a host-guest complex, it is best to use a flexible host because it is beneficial to overcome energetic (entropy and enthalpy) costs associated with restricting itself to a single conformation which reduces the overall binding free energy[17].

With the rapid increase of global demand for energy, nuclear energy has attracted worldwide attention due to its advantages of safety, cleanness, low greenhouse gas emissions and price economy[18, 19]. However, the nuclear fuel processing and some nuclear accidents release large amounts of radioactive iodine isotopes (^{129}I and ^{131}I), which hinders the promotion of nuclear energy and poses severe challenges to modern science and technology[20]. Among the radioisotopes of iodine, ^{129}I is a long-life isotope with a half-life of 1.57×10^7 years. ^{131}I is a short life isotope with relatively short half-life (8.02 days). Both of them can accumulate biologically through the food chain, thus affecting the metabolism process of human body[21, 22]. The accidents at Chernobyl and Fukushima nuclear power plant prove that we still cannot control nuclear energy safely.

Received 29 May 2021; accepted 12 October 2021 (**CCDC 2086538**)
① This work was supported by the Beijing Natural Science Foundation of China (2212002), National Natural Science Foundation of China (21906002, 21471011), the Beijing Municipal Science and Technology Project (KM202010005010), the Beijing Municipal High Level Innovative Team Building Program (IDHT20180504) and the Beijing Outstanding Young Scientist Program (BJJWZYJH01201910005017)
② Corresponding authors. E-mail: selfassembly@bjut.edu.cn or hwma@bit.edu.cn

Therefore, it has become a hot topic for scientists to deal with radioactive iodine quickly and effectively[23].

In previous work, we synthesized a series of metal-organic macrocycles, cages and capsules, which show potential applications in the complexation of inorganic anions, optical sensing and catalysis[24-28]. In this work, we synthesized four water soluble metal-organic capsules (**1·4NO$_3^-$**, **2·4NO$_3^-$**, **3·6NO$_3^-$**, and **4·6NO$_3^-$**) synthesized by using amide based polypyrazole ligands and dipalladium corners. The introduction of amide groups into ^{1}H-pyrazole-based ligands not only enhances hydrogen bonding between hosts and guests, but also increases the flexibility of the receptor molecules. Moreover, aromatic metal constructs are directional, which can control the configuration of the hosts, enhance the electrostatic interaction, and form a $\pi\cdots\pi$ stacking mode. Therefore, all the four supramolecular assemblies have the properties of adsorbing iodine via halogen bonds, electrostatic interactions and other supramolecular interactions.

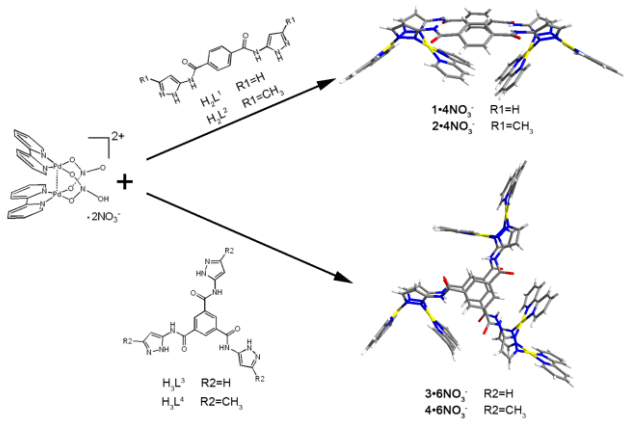

Scheme 1. Synthesis of compounds 1·4NO$_3^-$ ~ 4·6NO$_3^-$

2 EXPERIMENTAL

2. 1 Materials and methods

All the reagents viz. plladium(II) chloride, 2,2′-dipyridyl, silver nitrate, 1,4-dicarboxybenzene, trimesic acid, 3-aminopyrazole and 3-amino-5-methylpyrazole used were obtained from commercial suppliers and used as received. Acetone, thionyl chloride, N,N-dimethylformamide and acetonitrile were applied after redistilling. Deionized water was obtained by distillation using the ultrapure water mechanism of the best series laboratory. ^{1}H NMR spectra of all compounds were carried out on a Bruker 400 MHz spectrometer in DMSO-d_6 solution with TMS as internal standard at room temperature. Mass spectra were recorded on a JEOL Accu-TOF-4G LC-plus mass spectrometer. Elemental analyses (C, H and N) were carried out using German Elementar Vario Macro cube Analyzer. FT-IR spectra were recorded in a PerkinElmer spectrum two infrared spectrometer in the mid-IR region (4000 to 500 cm^{-1}). UV-vis spectra were carried out on a UV-2600 UV-vis. spectrophotometer with a 0.5 nm slit width. And thermogravimetric studies (25～800 ℃) were carried out using Labsys Evo Thermal Analyzer at a heating rate of 10 ℃ min^{-1}.

2. 2 Syntheses

The ligands H_2L^1, H_2L^2, H_3L^3 and H_4L^3, and the cages of **1·4NO$_3^-$～4·6NO$_3^-$** were synthesized by a same method as our previous work[29].

2. 2. 1 Synthesis of 1·4NO$_3^-$

A mixture of H_2L^1 (29.5 mg, 0.1 mmol) and $[(bpy)_2Pd_2(NO_3)_2](NO_3)_2$ (78 mg, 0.1 mmol) was stirred vigorously in 6 mL H_2O at room temperature for 3 hours, and then 5 mL acetone was added. The mixture was stirred for another hour at room temperature, and the solution became clear. Then, the mixture was removed to the oil-bath of 60 ℃ and continued stirring overnight. ^{1}H NMR spectroscopy confirmed quantitative formation of $\{[(bpy)_2Pd_2]_2L^1{}_2\}(NO_3)_4$ (**1 4NO$_3^-$**). Yield: 90%. ^{1}H NMR (400 MHz, DMSO-d_6, 300 K): δ 11.06 (s, 2H), 10.91 (s, 2H), 8.73 (d, 4H), 8.57 (d, 4H), 8.48 (t, 4H), 8.39~8.30 (m, 8H), 8.00~7.98 (m, 8H), 7.86~7.83 (m, 12H), 7.71~7.65 (m, 4H), 6.73 (d, 2H), 6.70 (d, 2H). Anal. Calcd. for $[C_{68}H_{52}N_{24}O_{16}Pd_4]$: C, 43.28; H, 2.78; N, 17.81. Found: C, 43.31; H, 2.75; N, 17.76.

2. 2. 2 Synthesis of 2·4NO_3^-

Compound {[$(bpy)_2Pd_2]_2L^2_2$}$(NO_3)_4$ (**2·4NO_3^-**) was synthesized by a similar method as **1·4NO_3^-**. Yield: 94%. ^{1}H NMR (400 MHz, DMSO-d_6, 300K): δ 10.91~10.80 (d, 4H), 8.75~8.72 (m, 4H), 8.56 (t, 4H), 8.48~8.43 (m, 4H), 8.36~8.29 (m, 4H), 8.20 (d, 4H), 8.11 (t, 4H), 7.92 (s, 3H), 7.83 (s, 5H), 7.80~7.76 (m, 4H), 7.69~7.65 (m, 4H), 6.54~6.49 (d, 4H), 2.42 (d, 12H). Anal. Calcd. (%) for [$C_{72}H_{60}N_{24}O_{16}Pd_4$]: C, 44.51; H, 3.11; N, 17.30. Found (%): C, 44.56; H, 3.05; N, 17.41.

2. 2. 3 Synthesis of 3·6NO_3^-

A mixture of H_3L^3 (40.5 mg, 0.1 mmol) and $[(bpy)_2Pd_2(NO_3)_2](NO_3)_2$ (116 mg, 0.15 mmol) was stirred vigorously in 6 mL H_2O at room temperature for 3 hours, and then 5 mL acetone was added. The mixture was stirred for another hour at room temperature. Then, the mixture was removed to the oil-bath of 60 ℃ and continued stirring overnight. ^{1}H NMR spectroscopy confirmed quantitative formation of {[$(bpy)_2Pd_2]_3L^3_2$}$(NO_3)_6$ (**3·6NO_3^-**). The resulting solution was allowed to stand for several days during which pale yellow crystals of the products along with the co-crystallized solvent water molecules were formed (**3·3.5NO_3^-·4O_2**). Yield: 90%. ^{1}H NMR (400 MHz, DMSO-d_6, 300K): δ 10.76 (s, 6H), 8.74 (d, 6H), 8.51~8.44 (m, 18H), 8.38 (d, 6H), 8.03 (d, 6H), 7.93 (d, 6H), 7.84~7.78 (m, 12H), 7.18 (s, 6H), 6.76 (d, 6H). Anal. Calcd. (%) for [$C_{96}H_{72}N_{36}O_{24}Pd_6$]: C, 41.89; H, 2.64; N, 18.32. Found (%): C, 41.90; H, 2.57; N, 18.28.

2. 2. 4 Synthesis of 4·6NO_3^-

The self-assembly of **4·6NO_3^-**: compound {[$(bpy)_2Pd_2]_3L^4_2$}$(NO_3)_6$ (**4·6NO_3^-**) was synthesized by a similar method as **3·6NO_3^-**.

4·6NO_3^-: yield: 91%. ^{1}H NMR (400 MHz, DMSO-d_6, 300K): δ 10.66 (s, 6H), 8.71~8.69 (d, 6H), 8.54~8.52 (d, 6H), 8.43 (m, 12H), 8.22~8.21 (d, 6H), 8.17~8.15 (d, 6H), 7.78~7.72 (m, 12H), 7.38 (m, 6H), 6.45 (m, 6H), 2.38 (s, 18H). Anal. Calcd. (%) for [$C_{102}H_{84}N_{36}O_{24}Pd_6$]: C, 43.19; H, 2.98; N, 17.78. Found (%): C, 43.23; H, 2.95; N, 17.69.

2. 3 X-ray data collection and structure refinement

Data collections were performed at 150 K for **3·3.5NO_3^-·4O_2** on a Bruker Smart APEX II CCD diffractometer equipped with graphite-monochromated Mo$K\alpha$ radiation (λ = 0.71073 Å). The absorption correction was performed using SADABS. The structure was solved by direct methods and refined employing full-matrix least-squares on F^2 by using the SHELXTL (Bruker, 2000) software program and expanded using Fourier techniques. All non-H atoms of the compounds were refined with anisotropic thermal parameters. The hydrogen atoms were included in idealized positions. The final residuals along with unit cell, space group, data collection, and refinement parameters are presented in Tables S1-S2.

2. 4 Host-guest study for compounds 1·4NO_3^-～4·6NO_3^- with iodine molecules

Pale yellow powders of compounds **1·4NO_3^-～4·6NO_3^-** were dried in a programmable oven at 60 ℃ for 24 h. The powder (30～40 mg) with its weight exactly measured was immersed in the n-hexane solutions (5 mL) containing iodine molecules for 24 h at 25 ℃. The process of iodine adsorption by compounds **1·4NO_3^-** ～ **4·6NO_3^-** was monitored by visual photos and UV-vis. The structures of compounds **1·4NO_3^-**, **2·4NO_3^-** and **4·6NO_3^-** adsorbed iodine were determined by ^{1}H NMR. The adsorbed amount of iodine into the porous solids was estimated by electrospray ionization mass spectrometry (ESI-MS), thermogravimetric analysis (TGA), infrared spectrum (IR) and UV/vis spectroscopy.

3 RESULTS AND DISCUSSION

3. 1 Crystal structure of 3·3.5NO_3^-·4O_2

The structural analysis showed that compound **3·3.5NO_3^-·4O_2** crystallizes in monoclinic space group $P2_1/c$. It clearly shows that compound **3·3.5NO_3^-·4O_2** consists of two deprotonic ligand L^3 and three dipalladium corners, displaying a drum-like cage conformation at the center of compound **3·3.5NO_3^-·4O_2**, and the distance between the upper and lower sides of the drum (The distance between the benzene rings of the two ligands) is about 6.07 Å. The opening of the three dipalladium corners faced in the same direction, the arrangement in space formed a propeller shape (Fig. 1), the dihedral angles of the dipalladium corners are 83.74°, 79.10° and 80.65°, respectively, and the distances between Pd⋯Pd of each dipalladium corner are 3.26, 3.28 and 3.19 Å, respectively, which is in the range of typical Pd⋯Pd interactions (2.60～3.30 Å), suggesting the presence of weak metal-metal interactions. Interestingly, two nitrate anions are encapsulated in the cage via N–H⋯O hydrogen bonding interactions. One of the nitrate anions is located between the benzene rings of the two ligands and forms a nearly parallel configuration with the two benzene rings (The dihedral angles between the nitrate and the two

benzene rings are 1.77 ° and 4.68 °, respectively) via anion-π interactions. The distances between the nitrate and the two benzene rings are 3.08 and 3.17 Å, respectively. Simultaneously, the distances of N–H ··O hydrogen bonds between the nitrate anion and the amide group are 2.15 and 2.09 Å, respectively. While another nitrate anion located in the cavity forms a nearly vertical structure with the benzene rings of the ligands, and the dihedral angles between the nitrate and the two benzene rings are 88.69 ° and 89.80 °, respectively. Meanwhile, the nitrate anion forms an almost parallel configuration with 2,2′-bipyridine of a dipalladium corner through anion-π interactions. The dihedral angle between the nitrate and 2,2′-bipyridine is 8.44 °. Similarly, hydrogen bonds are also built by the nitrate anion and amide NH groups, and the distances between N–H ··O are 2.23 and 2.13 Å, respectively. There are a lot of water molecules in the crystal lattice (Fig. S20). The molecule cage of **3** is stacked into an original 1-D infinite chain via *b*-axis by $\pi \cdots \pi$ stacking interactions, while the structure of **3·3.5NO_3^-·4O_2** forms a grid framework via *c*-axis by $\pi \cdots \pi$ stacking interactions, as shown in Fig. 2. The intermolecular π-stacking interaction is shaped by the benzene rings of the ligands and the outside 2,2′-bipyridine moieties from the adjacent molecules. The distance between the benzene rings and the adjacent 2,2′-bipyridine moieties ($\pi \cdots \pi$ distance) is about 3.51 Å, while the $\pi \cdots \pi$ distance of the outside 2,2′-bipyridine moieties from the adjacent molecules is about 3.30 Å.

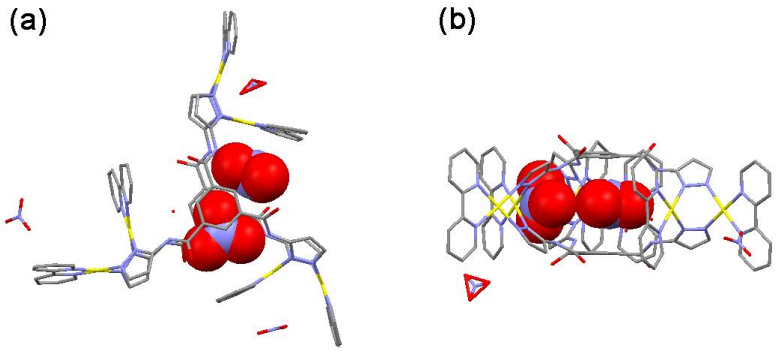

Fig. 1. Crystal structure of compound 3·3.5NO_3^-·4O_2 with hydrogen bonds. (a) Top view and (b) side view of the molecular structure. All the other residual molecules were omitted for clarity (yellow: Pd(II); gray: C; blue: N; red: O; white: H)

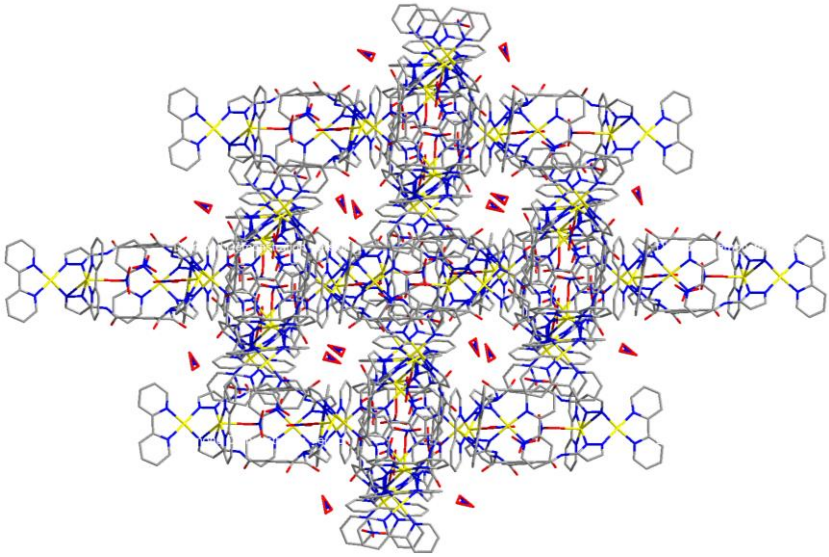

Fig. 2. Stacking crystal structure of compound 3·3.5NO_3^-·4O_2 (a) along the *b*-axis and (b) along the *c*-axis. All the other residual molecules were omitted for clarity (yellow: Pd(II); gray: C; blue: N; red: O; white: H)

3. 2 Study on the adsorption of iodine molecules by compounds $1{\cdot}4NO_3^-$～$4{\cdot}6NO_3^-$

As compounds $\mathbf{1{\cdot}4NO_3^-}$, $\mathbf{2{\cdot}4NO_3^-}$, $\mathbf{3{\cdot}6NO_3^-}$ and $\mathbf{4{\cdot}6NO_3^-}$ all held stable cage-like structures, an I_2 absorption study has thus been performed on powder samples of these compounds at room temperature. To put 30 mg $\mathbf{1{\cdot}4NO_3^-}$ powder into the n-hexane solution of iodine, it is very obvious that the color of the solution changed from purplish red to colorlessness which can be easily detected by the naked eye, as shown in Fig. 3. And the color of $\mathbf{1{\cdot}4NO_3^-}$ powder was changed from light yellow to dark red, which indicates the absorption properties of $\mathbf{1{\cdot}4NO_3^-}$ and its potential applications in removing radioactive iodine isotopes (^{129}I and ^{131}I) that are liberated during nuclear fuel treatment. To investigate the kinetics of I_2 adsorption of $\mathbf{1{\cdot}4NO_3^-}$, in situ UV/vis spectrum was recorded at room temperature. The visible absorption curve of n-hexane decreases with time. During the experiment, no further change was observed after 24 hours. The amount of I_2 loading of $I_2@\mathbf{1{\cdot}4NO_3^-}$ was 13.5% by weighing method. ^{1}H NMR spectra were analyzed to investigate the iodine loading (Fig. 4a). It clearly showed that no significant change was observed after adsorbing I_2, so the compound $\mathbf{1{\cdot}4NO_3^-}$ remained undamaged. Importantly, the ^{1}H NMR spectra of compound $I_2@\mathbf{1{\cdot}4NO_3^-}$ showed that compound $\mathbf{1{\cdot}4NO_3^-}$ still encapsulated a nitrate anion unsymmetrically after adsorbing iodine. In addition, the powder X-ray diffraction (XRD) spectra of $\mathbf{1{\cdot}4NO_3^-}$ and $I_2@\mathbf{1{\cdot}4NO_3^-}$ also demonstrated that the structure of compound $\mathbf{1{\cdot}4NO_3^-}$ after and before adsorption of iodine is consistent with each other (Fig. S1). Therefore, it can be inferred that compound $\mathbf{1{\cdot}4NO_3^-}$ adsorbs iodine through supramolecular interactions such as halogen bond and electrostatic interaction. In addition, in ESI-MS experiments, the peak present at 881.49 showed the molecular ion peak of $[\mathbf{1{\cdot}2NO_3^-}]^{2+}$. After adsorbing a molecule of iodine, the molecular weight (molecular formula: $C_{68}H_{52}N_{24}O_{16}Pd_4I_2$) was 2140.78, and ESI-MS peak present at 1008.00 (Fig. 4b) clearly showed that a molecule of iodine is adsorbed by a molecule of $\mathbf{1{\cdot}4NO_3^-}$. And thermogravimetric analysis (TGA) was also carried out to study the thermal stability and the incorporation percentage of guest molecules in $I_2@\mathbf{1{\cdot}4NO_3^-}$ (Fig. 4c). These results are in accordance with the above data, which indicated that iodine is adsorbed by intermolecular weak interaction with $\mathbf{1{\cdot}4NO_3^-}$, which is further evidenced by infrared data (Fig. 4d). Similarly, $\mathbf{2{\cdot}4NO_3^-}$, $\mathbf{3{\cdot}6NO_3^-}$ and $\mathbf{4{\cdot}6NO_3^-}$ also have the properties of adsorbing iodine via supramolecular interactions, and the amount of I_2 loading was 11.6%, 8.4%, and 8.2%, respectively (Fig. S2-S19).

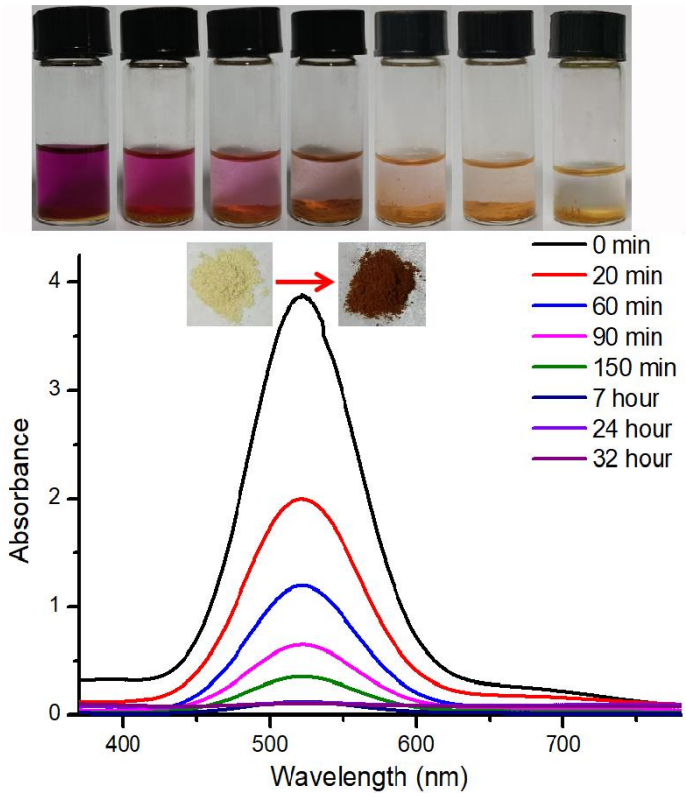

Fig. 3. Photographs showing the color change when 1 $4NO_3^-$ was soaked in n-hexane solution of I_2, and the UV/vis spectra of n-hexane solution of I_2 with 1 $4NO_3^-$ soaked in for the adsorbing process of iodine (Inset shows the photographs of 1 $4NO_3^-$ before and after I_2 adsorption)

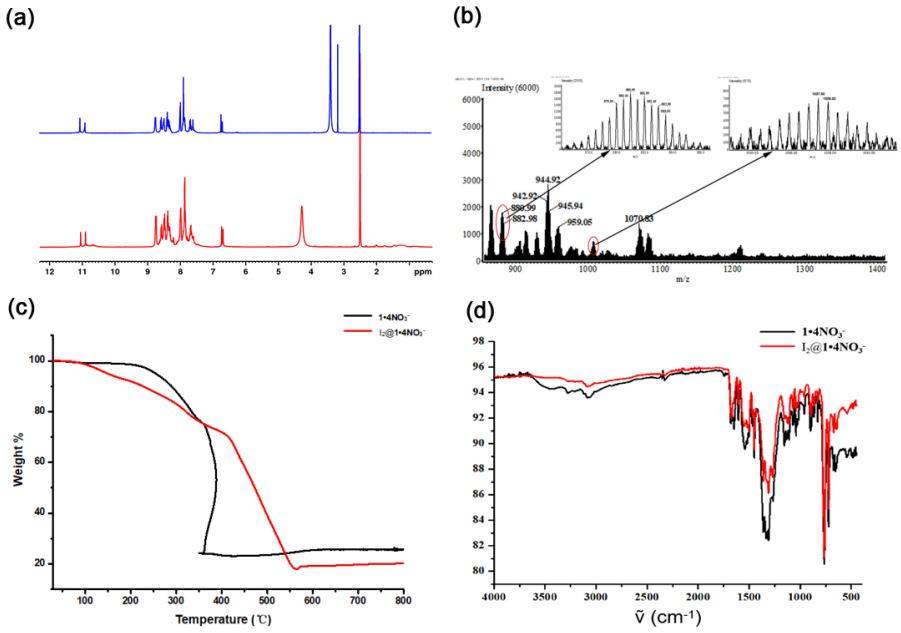

Fig. 4. (a) ^{1}H NMR spectra (400 MHz, 300 K, DMSO-d_6) of complex $1{\cdot}4NO_3^-$ before (blue) and after (red) iodine adsorption. (b) ESI-MS spectra of $I_2@1{\cdot}4NO_3^-$. (c) TGA curves of $1{\cdot}4NO_3^-$ and $I_2@1{\cdot}4NO_3^-$. (d) IR spectra of $1{\cdot}4NO_3^-$ and $I_2@1{\cdot}4NO_3^-$

4 CONCLUSION

In summary, we have synthesized four metal-organic molecular cages **$1{\cdot}4NO_3^-$**, **$2{\cdot}4NO_3^-$**, **$3{\cdot}6NO_3^-$**, and **$4{\cdot}6NO_3^-$** from coordination-driven self-assembly of the flexible amide-based polypyrazole ligands and dipalladium corners. These water-soluble compounds were characterized in both solution (NMR, ESI-MS) and solid state (X-ray single-crystal diffraction, TGA and infrared spectrum). Interestingly, all the four supramolecular assemblies are capable of adsorbing iodine through halogen bonds, electrostatic interactions and other supramolecular interactions.

REFERENCES

(1) Harris, K.; Fujita, D.; Fujita, M. Giant hollow M_nL_{2n} spherical complexes: structure, functionalisation and applications. *Chem. Commun*. **2013**, 49, 6703–6712.

(2) Hong, C. M.; Bergman, R. G.; Raymond, K. N.; Toste, F. D. Self-assembled tetrahedral hosts as supramolecular catalysts. *Acc. Chem. Res*. **2018**, 51, 2447–2455.

(3) Fiedler, D.; Leung, D. H.; Bergman, R. G.; Raymond, K. N. Selective molecular recognition, C−H bond activation, and catalysis in nanoscale reaction vessels. *Acc. Chem. Res*. **2005**, 38, 349–358.

(4) Liu, S.; Han, Y. F.; Jin, G. X. Formation of direct metal-metal bonds from 16-electron “pseudo-aromatic” half-sandwich complexes Cp″M[$E_2C_2(B_{10}H_{10})$]. *Chem. Soc. Rev*. **2007**, 36, 1543–1560.

(5) Lehn, J. M.; Rigault, A.; Siegel, J.; Harrowfield, J.; Chevrier, B.; Moras, D. Spontaneous assembly of double-stranded helicates from oligobipyridine ligands and copper(I) cations: structure of an inorganic double helix. *Proc. Natl. Acad. Sci. U. S. A*. **1987**, 84, 2565–2569.

(6) Scheer, M. The coordination chemistry of group 15 element ligand complexes - a developing area. *Dalton Trans*. **2008**, 4372–4386.

(7) Han, M.; Engelhard, D. M.; Clever, G. H. Self-assembled coordination cages based on banana-shaped ligands. *Chem. Soc. Rev*. **2014**, 43, 1848–1860.

(8) Takeda, N.; Umemoto, K.; Yamaguchi, K.; Fujita, M. A nanometre-sized hexahedral coordination capsule assembled from 24 components. *Nature* **1999**, 398, 794–796.

(9) Hong, M.; Zhao, Y.; Su, W.; Cao, R.; Fujita, M.; Zhou, Z.; Chan, A. S. C. A Nanometer-sized metallosupramolecular cube with O_h symmetry. *J. Am. Chem. Soc*. **2000**, 122, 4819–4820.

(10) Newkome, G. R.; He, E.; Moorefield, C. N. Suprasupermolecules with novel properties: metallodendrimers. *Chem. Rev*. **1999**, 99, 1689–1746.

(11) Amoroso, A. J.; Jeffery, J. C.; Jones, P. L.; McCleverty, J. A.; Thornton, P.; Ward, M. D. Self-assembly of a ferromagnetically coupled manganese(II)

tetramer. *Angew. Chem. Int. Ed*. **1995**, 34, 1443–1446.

(12) Argent, S. P.; Adams, H.; Riis-Johannessen, T.; Jeffery, J. C.; Harding, L. P.; Ward, M. D. High-nuclearity homoleptic and heteroleptic coordination cages based on tetra-capped truncated tetrahedral and cuboctahedral metal frameworks. *J. Am. Chem. Soc*. **2006**, 128, 72–73.

(13) Paul, R. L.; Bell, Z. R.; Jeffery, J. C.; Harding, L. P.; McCleverty, J. A.; Ward, M. D. Complexes of a bis-bidentate ligand with d10 ions: a mononuclear complex with Ag(I), and a tetrahedral cage complex with Zn(II) which encapsulates a fluoroborate anion. *Polyhedron* **2003**, 22, 781–787.

(14) Lehn, J. M. (Nobel Lecture) Supramolecular chemistry-scope and perspectives molecules, supermolecules, and molecular devices. *Angew. Chem. Int. Ed*. **1988**, 27, 89–112.

(15) Steed, J. W.; Atwood, J. L. Supramolecular chemistry, 2nd ed. John Wiley & Sons, Ltd. **2009**.

(16) Lehn, J. M. Supramolecular chemistry: where from? where to? *Chem. Soc. Rev.* **2017**, 46, 2378–2379.

(17) Oshovsky, G. V.; Reinhoudt, D. N.; Verboom, W. Supramolecular chemistry in water. *Angew. Chem. Int. Ed*. **2007**, 46, 2366–2393.

(18) Lin, Y.; Jiang, X.; Kim, S. T.; Alahakoon, S. B.; Hou, X.; Zhang, Z.; Thompson, C. M.; Smaldone, R. A.; Ke, C. An elastic hydrogen-bonded cross-linked organic framework for effective iodine capture in water. *J. Am. Chem. Soc*. **2017**, 139, 7172–7175.

(19) Riley, B. J.; Vienna, J. D.; Strachan, D. M.; McCloy, J. S.; Jerden, J. L. Materials and processes for the effective capture and immobilization of radioiodine: a review. *J. Nucl. Mater*. **2016**, 470, 307–326.

(20) Garcia, M. D.; Marti-Rujas, J.; Metrangolo, P.; Peinador, C.; Pilati, T.; Resnati, G.; Terraneo, G.; Ursini, M. Dimensional caging of polyiodides: cation-templated synthesis using bipyridinium salts. *CrystEngComm.* **2011**, 13, 4411–4416.

(21) Svensson, P. H.; Gorlov, M.; Kloo, L. Dimensional caging of polyiodides. *Inorg. Chem.* **2008**, 47, 11464–11466.

(22) Blake, A. J.; Devillanova, F. A.; Gould, R. O.; Li, W. S.; Lippolis, V.; Parsons, S.; Radek, C.; Schroder, M. Template self-assembly of polyiodide networks. *Chem. Soc. Rev*. **1998**, 27, 195–206.

(23) Kosaka, K.; Asami, M.; Kobashigawa, N.; Ohkubo, K.; Terada, H.; Kishida, N.; Akiba, M. Removal of radioactive iodine and cesium in water purification processes after an explosion at a nuclear power plant due to the Great East Japan Earthquake. *Water Res*. **2012**, 46, 4397–4404.

(24) Yu, S. Y.; Huang, H.; Liu, H. B.; Chen, Z. N.; Zhang, R.; Fujita, M. Modular cavity-tunable self-assembly of molecular bowls and crowns as structural analogues of calix[3]arenes. *Angew. Chem. Int. Ed.* **2003**, 42, 686–690.

(25) Xie, T. Z.; Guo, C.; Yu, S. Y.; Pan, Y. J. Fine-tuning conformational motion of a self-assembled metal-organic macrocycle by multiple C–H···anion hydrogen bonds. *Angew. Chem. Int. Ed*. **2012**, 51, 1177–1181.

(26) Jiang, X. F.; Hau, F. K. W.; Sun, Q. F.; Yu, S. Y.; Yam, V. W. W. From $\{Au^{I}\cdots Au^{I}\}$-coupled cages to the cage-built 2-D $\{Au^{I}\cdots Au^{I}\}$ arrays: $Au^{I}\cdots Au^{I}$ bonding interaction driven self-assembly and their Ag^{I} sensing and photo-switchable behavior. *J. Am. Chem. Soc*. **2014**, 136, 10921–10929.

(27) Jiang, X. F.; Huang, H.; Chai, Y. F.; Lohr, T. L.; Yu, S. Y.; Lai, W.; Pan, Y. J.; Delferro, M.; Marks, T. J. Hydrolytic cleavage of both CS_2 carbon-sulfur bonds by multinuclear Pd(II) complexes at room temperature. *Nat. Chem.* **2017**, 9, 188–193.

(28) Deng, W.; Yu, Z. S.; Ma, H. W.; Yu, S. Y. Self-assembly of water-soluble platinum(II)-based metallacalixarenes and tuning their conformational interconversion via synergistic effects between solvents and anions. *Chem. Asian J*. **2018**, 13, 2805–2811.

(29) Lu, H. L.; Tong, J.; Hu, X. P.; Deng, W.; Yu, S. Y. Dipalladium(Ⅱ,Ⅱ)-assembled molecular capsules that unsymmetrically encapsulate a nitrate via hydrogen bonding. *Inorg. Chem. Commun*. DOI: 10.1016/j.inoche.2021.108672.